Edinburgh Research Explorer

Glioma stem cell lines expanded in adherent culture have tumor-specific phenotypes and are suitable for chemical and genetic screens

Glioma Stem Cell Lines Expanded in Adherent Culture Have Tumor-Specific Phenotypes and Are Suitable for Chemical and Genetic Screens

Steven M. Pollard,[1,7,*] Koichi Yoshikawa,[2,7] Ian D. Clarke,[2] Davide Danovi,[1] Stefan Stricker,[1] Roslin Russell,[1] Jane Bayani,[4] Renee Head,[2] Marco Lee,[3] Mark Bernstein,[5] Jeremy A. Squire,[6] Austin Smith,[1] and Peter Dirks[2,*]

[1]Wellcome Trust Centre for Stem Cell Research and Department of Biochemistry, University of Cambridge, Tennis Court Road, Cambridge CB2 1QR, UK
[2]Arthur and Sonia Labatt Brain Tumor Research Center, Program in Developmental and Stem Cell Biology, The Hospital for Sick Children, University of Toronto, 555 University Avenue, Toronto, Ontario M5G 1X8, Canada
[3]Division of Clinical Neurosciences, Western General Hospital, Edinburgh EH4 2XU, UK
[4]Department of Applied Molecular Oncology, Ontario Cancer Institute, University Health Network, University of Toronto, 610 University Avenue, Toronto, Ontario M5G 2M9, Canada
[5]Division of Neurosurgery, Toronto Western Hospital, University of Toronto, 399 Bathurst Street, Toronto, Ontario M5T 2S8, Canada
[6]Department of Pathology and Molecular Medicine, Richardson Building, Stuart Street, Queen's University, Kingston, Ontario K7L 3N6, Canada
[7]These authors contributed equally to this work
*Correspondence: steve.pollard@cscr.cam.ac.uk (S.M.P.), peter.dirks@sickkids.ca (P.D.)
DOI 10.1016/j.stem.2009.03.014

SUMMARY

Human brain tumors appear to have a hierarchical cellular organization suggestive of a stem cell foundation. In vitro expansion of the putative cancer stem cells as stable cell lines would provide a powerful model system to study their biology. Here, we demonstrate routine and efficient derivation of adherent cell lines from malignant glioma that display stem cell properties and initiate high-grade gliomas following xenotransplantation. Significantly, glioma neural stem (GNS) cell lines from different tumors exhibit divergent gene expression signatures and differentiation behavior that correlate with specific neural progenitor subtypes. The diversity of gliomas may, therefore, reflect distinct cancer stem cell phenotypes. The purity and stability of adherent GNS cell lines offer significant advantages compared to "sphere" cultures, enabling refined studies of cancer stem cell behavior. A proof-of-principle live cell imaging-based chemical screen (450 FDA-approved drugs) identifies both differential sensitivities of GNS cells and a common susceptibility to perturbation of serotonin signaling.

INTRODUCTION

The most common and aggressive type of primary adult brain cancer is malignant glioma. Current treatments for these cancers are largely ineffective. Gliomas are classified as astrocytoma, oligodendroglioma, or ependymoma, based on the glial cell type that predominates in the tumor (Kleihues and Cavenee, 2000). Glioblastoma multiform (GBM) is the most common and aggressive form of malignant astrocytoma and can arise de novo or

from pre-existing lower-grade tumors (Kleihues and Cavenee, 2000). Molecular profiling of GBM tumors has suggested distinct subclasses of the disease (Mischel et al., 2003; Louis, 2006; Phillips et al., 2006). However, individual tumors contain varying proportions of apparently differentiated cell types, alongside ill-defined anaplastic cells, which complicates accurate diagnosis and grading. Though there has been success in identifying the disrupted signaling pathways and underlying genetic defects associated with glial tumors (Furnari et al., 2007; Cancer Genome Atlas Research Network, 2008), it remains unclear how these operate in different cellular contexts.

It is possible that cellular heterogeneity within each tumor arises from cells that display stem cell characteristics—namely, long-term self-renewal and capacity to differentiate, as previously demonstrated for leukemia (Lapidot et al., 1994). Such stem cells would underlie a cellular hierarchy and drive tumor growth through sustained self-renewal. We, and others, have shown that a subpopulation of putative cancer stem cells can be isolated from diverse adult and childhood brain tumors using the neural stem cell marker CD133 (Hemmati et al., 2003; Singh et al., 2003), and these can initiate tumor formation following xenotransplantation (Singh et al., 2004). These data, together with similar approaches for other solid tumors, provide support for the cancer stem cell hypothesis (Reya et al., 2001; Ward and Dirks, 2007).

Establishing cell lines from tumors that retain cancer-initiating stem cell properties would provide a valuable and accurate model of the human disease. It would also give insight into the origin of tumor heterogeneity and enable more refined analysis of molecular mechanisms that regulate transformation, self-renewal, commitment, and differentiation. Together with complementary studies using mouse genetic models, these approaches should lead to more rational therapeutic strategies. The neurosphere culture paradigm has been used successfully for enrichment of tumor-initiating cells from brain tumors (Ignatova et al., 2002; Hemmati et al., 2003; Singh et al., 2003; Galli et al., 2004;

Yuan et al., 2004). Long-term expansion of neurospheres from GBM has, in some cases, been possible in serum-free media, and such cultures are an improvement on "classic" glioma cell lines, such as U87, or other serum-cultured lines, which fail to model accurately the human disease (Galli et al., 2004; Lee et al., 2006). However, neurosphere culture has several limitations. Short-lived progenitor cells also proliferate in suspension culture, and true clonal analysis is hampered by sphere aggregation (Suslov et al., 2002; Reynolds and Rietze, 2005; Singec et al., 2006). Most problematic is the spontaneous differentiation and cell death that accompany stem cell divisions in the sphere environment. This limits rigorous assessment of stem cell behavior and marker analysis based on bulk populations (Suslov et al., 2002). Thus, the true nature of the stem cell compartment across the spectrum of gliomas and their relationship to in vivo progenitors remain unclear (Stiles and Rowitch, 2008).

We recently reported methodology for deriving and expanding mouse and human adherent neural stem (NS) cell lines (Conti et al., 2005; Pollard et al., 2006; Sun et al., 2008). Adherent culture provides uniform access to growth factors, which suppresses differentiation and enables expansion of highly pure populations of stem cells. In this study, we investigated whether gliomas may yield glioma neural stem (GNS) cell lines in similar adherent culture conditions.

RESULTS

Adherent NS-like Cell Lines Can Be Established Readily from Human Gliomas

The key requirement for propagating both mouse and human NS cells without spontaneous differentiation or cell death is a combination of the growth factors EGF and FGF-2 on an adherent substrate (Conti et al., 2005; Sun et al., 2008). We tested whether these conditions enable the isolation and expansion of stem cells from gliomas. Glioma tissue was recovered following surgical procedures and was immediately processed (see Supplemental Experimental Procedures available online). Following direct plating onto a laminin-coated flask in NS cell culture media, we observed survival and establishment of primary cultures from all glioblastoma samples tested (Figure 1A). There is a diversity of cellular phenotypes within these initial cultures, reflecting mixtures of progenitors and differentiated cells together with putative stem cells.

For some samples, high levels of cell death within the tumor mass interfered with establishment of adherent cultures due to excessive cell debris binding to the substrate. In these instances, cells initially formed aggregates, or neurospheres. After 7–10 days, these were harvested free from dead cells and debris and allowed to settle and attach. NS cells grow out from these primary spheres (Figure 1A), as previously demonstrated for mouse and human NS cells (Conti et al., 2005; Sun et al., 2008). Using each of these derivation approaches, we are routinely able to generate adherent primary cultures of human malignant glioma cells.

Cultures expanded continuously with a doubling time of around 3–5 days. Within 2–3 passages, cultures became less heterogeneous. As for fetal NS cells, we find that a laminin substrate provides the most effective means to propagate the cells, while parallel cultures on gelatin or untreated plastic

undergo cell clumping, and cells detach (data not shown). Using these adherent conditions, we have been able to expand six cell lines for at least 1 year (>20 passages) without any obvious crisis or alteration in growth rate, although genetic alterations did occur at late passage (see below). Cell lines were established from histopathologically distinct types of tumor, namely three cases of glioblastoma multiforme (G144, G166, and GliNS2), a giant cell glioblastoma (G179), and an anaplastic oligoastrocytoma (G174). For one glioma sample (patient no. 144), we established cell lines independently in each of our laboratories using the same initial tumor sample. These cell lines were designated G144 and G144ED. In all subsequent analyses performed, we have found no striking differences in behavior or marker expression between these two cell lines.

To ascertain whether the glioma-derived cells have similarities to fetal NS cells (Sun et al., 2008), we undertook a phenotypic characterization of NS cell/neural progenitor cell markers. Immunocytochemistry confirmed that nearly all cells within the culture express Vimentin, Sox2, Nestin, CD44, and 3CB2, although for each of these, there appears to be some variations in levels between cells (Figure 1B and data not shown). By time-lapse videomicroscopy, it is apparent that cells within G144 and G179 cultures display dynamic changes in cell shape and are highly motile, both features of fetal NS cells (Movies S7 and S11). Quantitative data generated from cell tracking analysis identified that G166 cells are less motile than G144 cells, with the later moving on average 1.8 times further from their initial position (Movies S1–S4). Thus, glioma-derived cell lines are broadly similar to normal NS cells. Therefore, we term them glioma NS (GNS) cells. Each line can be efficiently recovered following freezing and thawing and can readily be genetically modified using nucleofection (see Supplemental Data).

To compare the efficiency with which adherent GNS cell lines can be established compared to suspension culture (sphere) methods, we performed side-by-side derivation for an additional six primary tumor samples (five GBMs and one anaplastic oligodendroglioma). The primary glioma cell population was split into two flasks, one coated with laminin and the other without (sphere conditions). Strikingly, using the adherent NS cell conditions, we were able to establish cultures from all six samples, and these were all expanded for at least 10 passages. By contrast, in suspension culture, although most samples generated spheres/aggregates upon initial plating, only two of these could be passaged further. For these two sphere cultures, we noted reduced expansion compared to side-by-side adherent cultures (passage 5 for each glioma sphere culture versus > passage 10 for all six adherent GNS cells).

Increased efficiency of establishing and propagating glioma cells in adherent conditions may be attributable to increased differentiation and apoptosis in sphere culture. This is analogous to the embryonic stem cell cultures that are maintained as pure stem cell cultures in adherent culture but undergo differentiation when plated in suspension, generating embryoid bodies (Doetschman et al., 1985). We compared the extent of differentiation and apoptosis in side-by-side cultures expanded either adherently or as spheres (Figure 2). This analysis was performed using established adherent lines to generate spheres (G144, G144-D6, and G179). As the initial starting cell population is the same, this experiment compares directly the effects of the
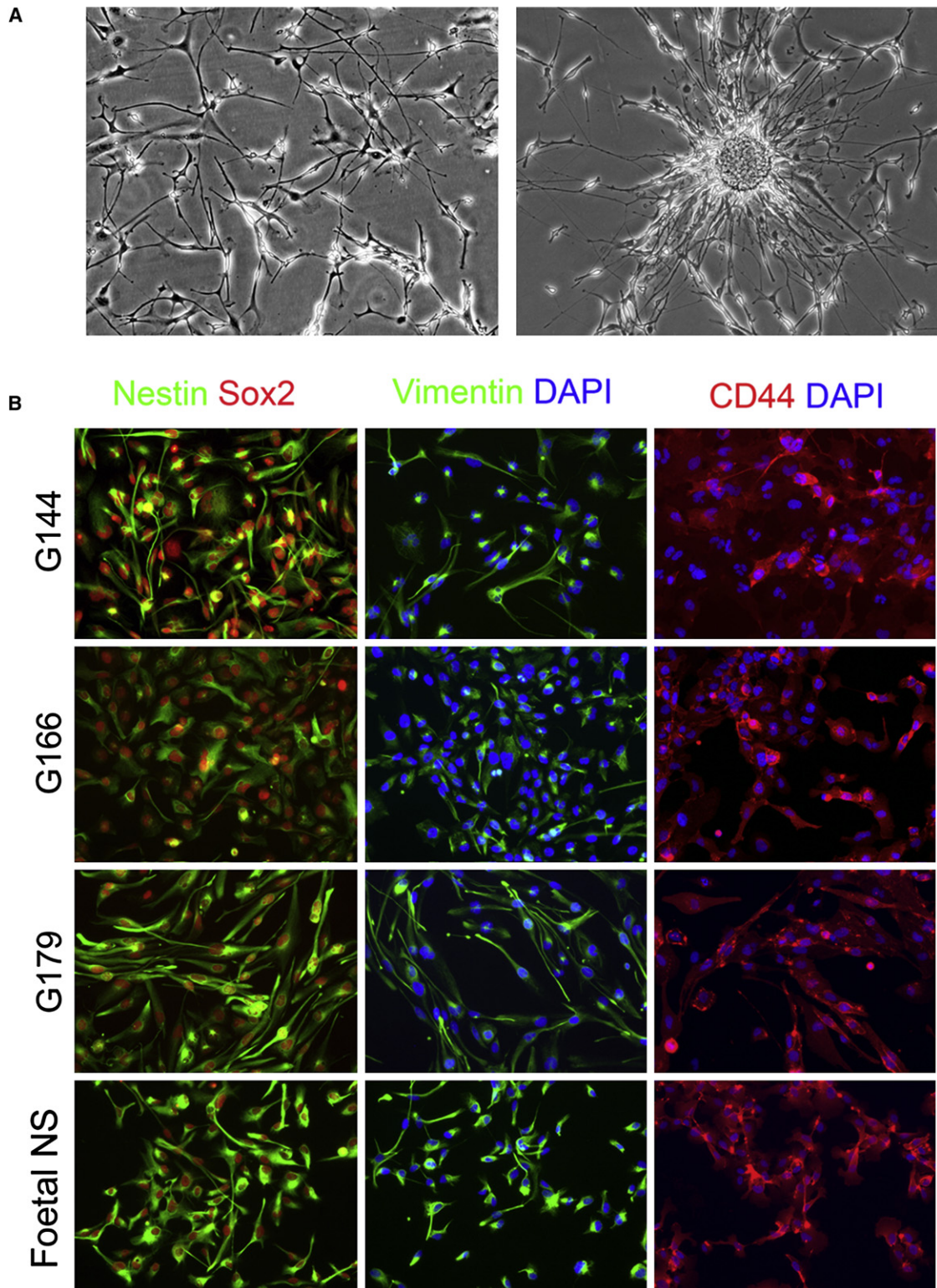
Figure 1. Derivation and Initial Characterization of GNS Cells

(A) Typical example of primary cultures established by plating of glioma tumor populations directly on a laminin substrate in NS cell expansion media (left) or briefly maintained in suspension and then plated in a laminin-coated flask (right).

(B) Immunostaining for the neural progenitor markers Nestin, Sox2, Vimentin, and CD44 in three different glioma cell lines (G144, G166, and G179) and one fetal NS cell line (CB541).
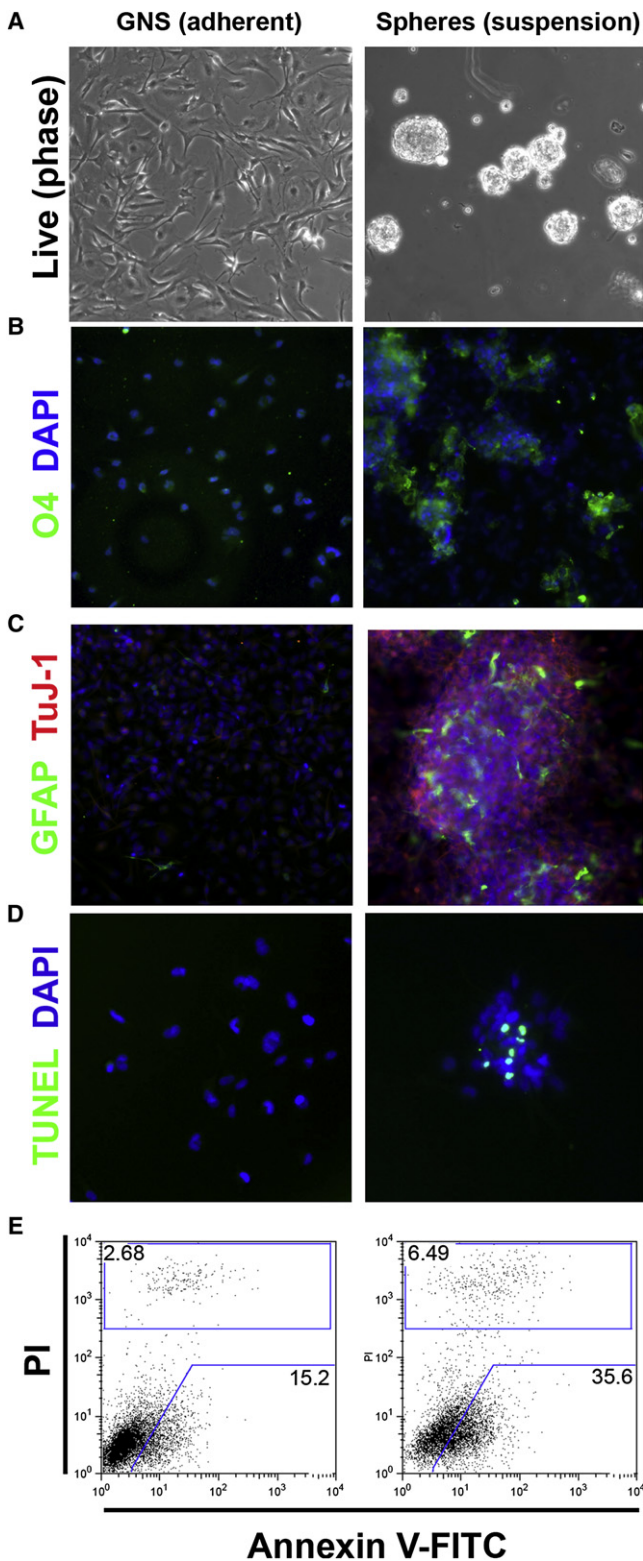
Figure 2. Elevated Differentiation and Cell Death in Sphere Cultures

Adherent GNS cells (the clonal line G144-D6) readily generated spheres when plated in suspension culture (A). After two passages in identical medium with EGF and FGF-2, immunocytochemistry was performed to assess differentiation to oligodendrocytes (B) or TuJ-1+ neurons and GFAP-expressing astro-

two culture regimes. Handling of cells, dissociation, staining, and media used were carried out in parallel. We found increased numbers of cells expressing differentiation markers in the spheres (GFAP, O4, and TuJ-1) (Figures 2B and 2C), as well as increased levels of cell death using the TUNEL assay and Annexin V staining (36% versus 15%) (Figures 2D and 2E). We also examined the cultures maintained continuously as spheres and their adherent counterparts and similarly found higher levels of differentiation markers in the spheres (Figure S1). Together, these findings indicate that monolayer culture enables routine expansion of glioma cells with reduced levels of differentiation and apoptosis. Three cell lines (G144, G166, and G179) are characterized in detail in this study.

Genomic Aberrations in GNS Cells

To determine whether GNS cells display genomic alterations characteristic of GBM, we performed molecular cytogenetic analyses using spectral karyotyping (SKY), locus-specific FISH, and comparative genomic hybridization (Figures S2 and S3). G144 cultures exhibited no aberrant chromosomes and contained a mixture of diploid (2n) and tetraploid (4n) cells. Simple numerical gains of chromosomes 7 and 19, together with loss of chromosomes 6, 8, and 15, were identified. With the exception of chromosome 8 deletion, each of these changes is commonly associated with glioblastoma (Cancer Genome Atlas Research Network, 2008; Parsons et al., 2008). Increased copy numbers of chromosome 7 were confirmed by EGFR-specific interphase FISH using tissue samples derived from the surgical resection of the tumor, as well as cultured cells (Figure S2). It is noteworthy that the *EGFR*, *CDK6*, and *MET* genes map to this chromosome. Comparative genomic hybridization for G144 revealed an amplification of the *CDK4* locus on chromosome 12 and deletion of *PTEN* on chromosome 10. Two clonal cell lines generated from the G144 population (expanded for more than 6 months) exhibited no major change from the parental population (Figure S3). However, late passage G144 (passage 50) cultures did show a more complex and heterogeneous pattern of both numerical and structural chromosomal change (Figure S2). Similarly, G179 exhibited a more complex chromosomal constitution at later passages, and similar to G144, polysomic gain of whole chromosome 7 was evident. Thus, although GNS cells do not display gross chromosome instability, alterations in whole chromosome copy number do occur following long-term in vitro expansion. Therefore, we routinely use cultures expanded for no more than 20 passages.

GNS Cell Lines Are Tumorigenic

To test the capacity of GNS cells to initiate tumor formation, we carried out intracranial transplantation into immunocompromised mice. Initially, we injected 100,000 cells from G144 cultures (expanded > 10 passages). After 5 weeks, a first cohort of mice was sacrificed and revealed large numbers of engrafted human nestin immunoreactive cells that had infiltrated the host brain (Figure S4). A second cohort of mice was sacrificed after

cytes (C). Cell death is higher within spheres than within adherent cultures, as determined by TUNEL (D) and Annexin V staining (E). Similar results were obtained for G144 and G179.
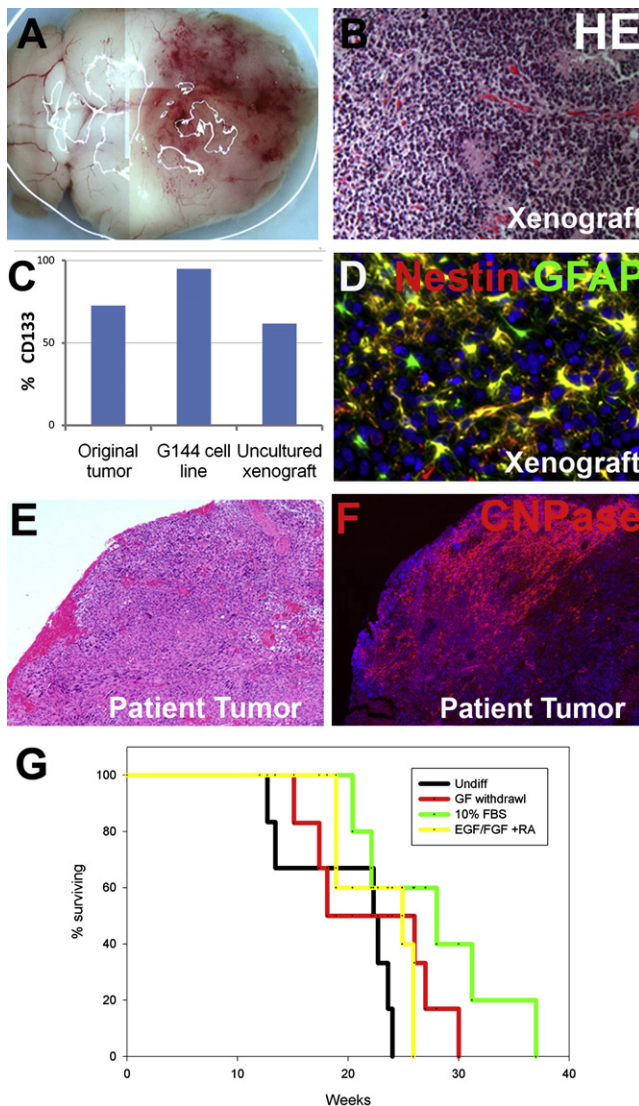
Figure 3. G144 Cells Generate Tumors following Xenotransplantation

(A) GNS cells that were transplanted into immunocompromised mice produced a large tumor mass (22 weeks after transplantation of 10^5 G144 cells, passage 18).

(B) A similar xenograft tumor sectioned and assessed for histopathology displayed hallmarks of GBM. HE, hematoxylin and eosin.

(C) Flow cytometry quantitation of CD133$^+$ cells within the directly harvested/uncultured xenograft compared to the original patient tumor.

(D) Immunocytochemistry for Nestin (red) and GFAP (green) in xenograft tumors.

(E) The original G144 patient tumor was graded as GBM. However, consistent with the G144 in vitro differentiation, CNPase$^+$ oligodendrocyte-like cells are widespread (F).

(G) Kaplan Meier plots for transplants of G144 cells exposed to each differentiation condition for 14 days prior to transplantation of 200,000 cells (n = 6 for condition).

20 weeks or longer. In these animals, we observed formation of large and highly vascularized tumors (Figure 3A).

The histopathology of these xenograft tumors is strikingly similar to human GBM tumors, namely pseudopalisading

necrosis, nuclear pleomorphism, and extensive microvascular proliferation (Kleihues and Cavenee, 2000) (Figures 3A and 3B). Cellular heterogeneity is evident within the xenograft tumor population upon immunostaining for Nestin and GFAP or flow cytometry for CD133 (Figures 3C and 3D). CD44 and Nestin-expressing tumor cells are frequently identified on the periphery of the tumors, with GFAP more prominent centrally, suggesting that the most primitive cells are invasive (Figure S5). Transplantation of G144 cells after exposure to differentiation-promoting conditions in vitro resulted in delayed tumor formation (Figure 3G).

G166 and G179, as well as two other GNS cell lines tested (G174 and GliNS2), also generated tumors (Figure 4A and Table S1). Highly infiltrative behavior characterizes high-grade glioma and makes full surgical resection of the tumor population impossible. In most transplants, we saw a striking infiltration of the brain reminiscent of the human disease. An exception was G166, which generated a more defined tumor mass (Figure 4A).

To calibrate tumor-initiating potency, we carried out transplantations using 10-fold dilutions of cells (n = 47). The minimum number of cells tested (100) resulted, in most cases, in cell engraftment and for two lines (G144 and G174) was sufficient to generate an aggressive tumor mass (Table S1). This is consistent with our previous findings with acutely isolated CD133$^+$ cells (Singh et al., 2004). G166 and G179 generated tumors using 1000 cells. Clonal expansion from a single G144 cell in vitro followed by transplantation also resulted in similar tumors (Figure S5). These results contrast sharply with normal fetal NS cells, which never generated tumors even using 10^5 cells (n = 5) (Figure 4A). To determine whether the tumor-initiating cells self-renew within the xenograft, we carried out serial transplantations from the tumor mass into secondary and tertiary recipients using G144 cells. In each case, tumors were generated (Figure 4B). Re-derivation of long-term expandable GNS cells from G144-ED and G179 xenograft tumors was also straightforward using adherent conditions. However, parallel cultures expanded using suspension culture methods failed to expand past passages 5 and 6, respectively. Together, these data demonstrate that long-term expanded glioma-derived stem cell lines remain highly tumorigenic and are capable of forming tumors that appear to recapitulate the human disease.

GNS Cell Lines Exhibit Distinct Differentiation Behaviors In Vitro

A defining property of stem cells is their ability to generate differentiated progeny. The most prevalent form of glioma is referred to as astrocytoma, based on the predominance of GFAP$^+$ astrocyte-like cells within the tumor mass. However, GBMs also contain anaplastic cell populations and, in some cases, an oligodendrocyte component (Kleihues and Cavenee, 2000).

For all GNS cells analyzed and in contrast to glioma neurospheres (Yuan et al., 2004), we find that differentiation to oligodendrocytes (O4$^+$) or neurons (TuJ-1$^+$) is fully suppressed in the presence of EGF and FGF-2 (Figure 5A). We tested the capacity of GNS cells to undergo oligodendrocyte or neuronal differentiation upon growth factor withdrawal. In contrast to fetal NS cells, G144 and G179 GNS cells did not undergo massive cell death in response to growth factor withdrawal but, instead, began to differentiate (Movies S5–S12). For G144, we noted the appearance of significant numbers of O4$^+$ or CNPase$^+$ oligodendrocyte-like cells

A

G144 (10000 cells) 24w

G166 (100000 cells) 22w

G174 (100 cells) 20w

G179 (100000 cells) 24w

Foetal NS (100000 cells) 20w

hNestin DAPI   hNestin DAPI

B

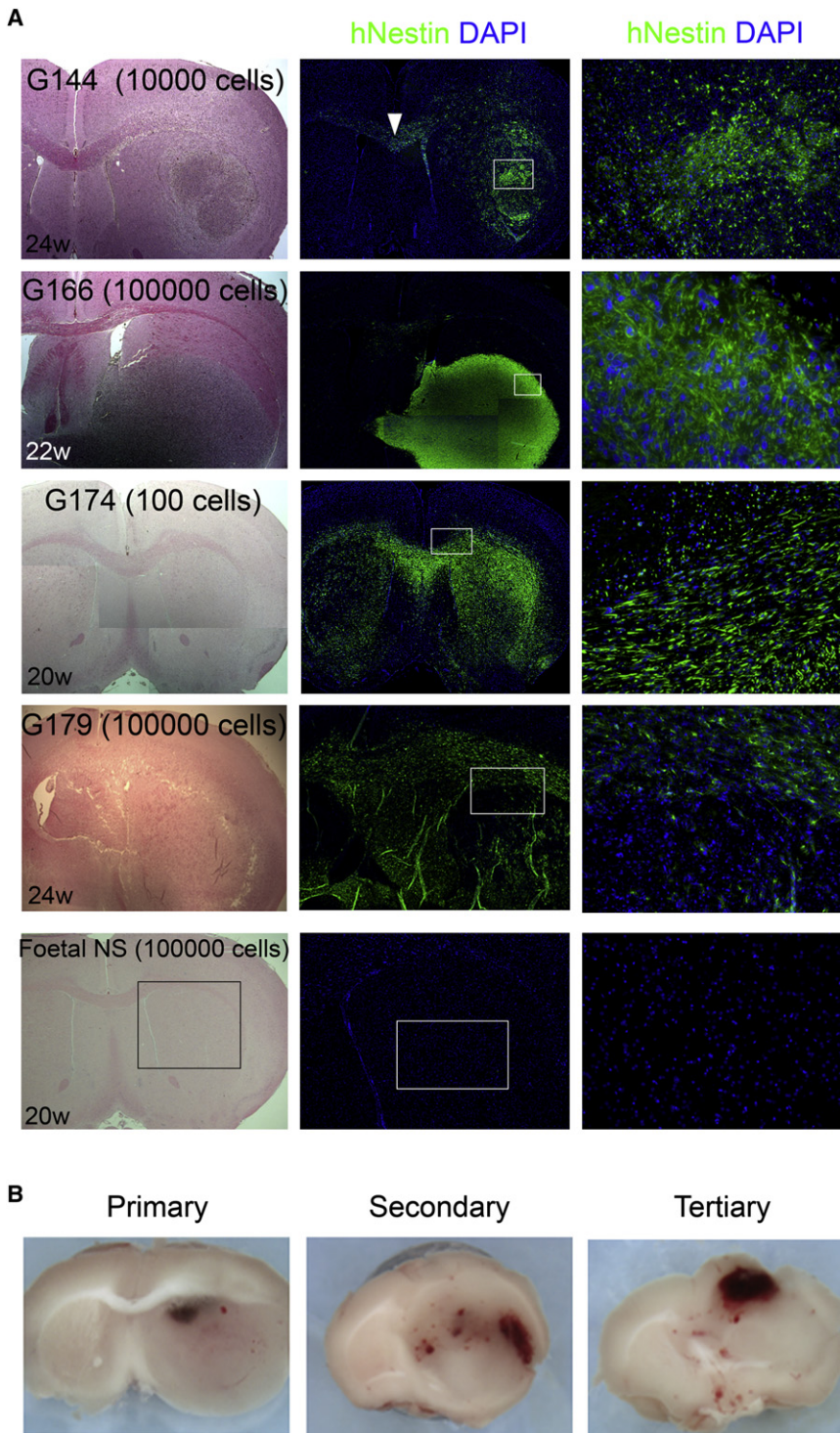Primary   Secondary   Tertiary

Figure 4. All GNS Cell Lines are Tumorigenic
(A) Xenotransplantation of each GNS cell line led to formation of a tumor mass with highly infiltrative behavior (arrow), except for G166. (Left) Coronal section of brain stained with H&E. (Right) Staining for human nestin (boxed region of middle panels). Foetal NS cells (hf240) fail to generate tumors.
(B) G144 xenograft-derived cells serially transplanted into secondary and tertiary hosts.

7 days following addition of BMP-4, we observed a striking change in cell morphology. The majority of cells expressed high levels of GFAP, although in each case, there was also a minor population of Doublecortin$^+$ (Dcx$^+$) neuronal-like cells (Figure 5C). This response is similar to that of human fetal NS cells (Sun et al., 2008). Similar results were seen upon serum treatment (data not shown). For G166, GFAP$^+$ cells were also observed, but only at low frequency. Thus, whereas GNS cells retain a capacity to differentiate, efficiency and lineage choice vary dramatically between each line.

GNS Cell Lines Have Properties Related to Specific Classes of Neural Progenitors

The tendency of G144 cells to differentiate into oligodendrocytes was surprising. For mouse and human fetal NS cells, efficient oligodendrocyte differentiation requires a stepwise differentiation protocol involving exposure to the exogenous signals, thyroid hormone, ascorbic acid, and PDGF and results in heterogeneous populations of neurons, astrocytes, and oligodendrocytes (Glaser et al., 2007; Sun et al., 2008). G144 cells may represent a corrupted tripotent state that has acquired genetic changes that influence the lineage choice during differentiation, biasing toward oligodendrocyte commitment. Alternatively, G144 cells may have a distinct phenotype more similar to oligodendrocyte precursor cells (OLPs) than to NS cells. To distinguish between these two possibilities, we assessed established markers of OLPs (Olig2, Sox10, NG2, and PDGFRα) to identify whether they are expressed prior to or during differentiation.

Using immunocytochemistry, we find that G144 cells, but not G166, G179, or human fetal NS cells, coexpress Sox10 and NG2 in proliferating conditions (Figure 6A). Quantitative RT-PCR confirmed that G144 cells express higher levels (>50-fold) of

within 1 week (Figure 5B and data not shown). By contrast, G179 mainly produced TuJ-1$^+$ cells (Figure 5B). Neuronal-like cells or oligodendrocytes were not apparent in G166 cultures, which continued to proliferate in the absence of EGF and FGF-2 without overt differentiation (Figure 5 and Movie S10).

To determine whether GNS cells could generate astrocytes, we exposed cells to BMP-4 or serum. For G144 and G179, within
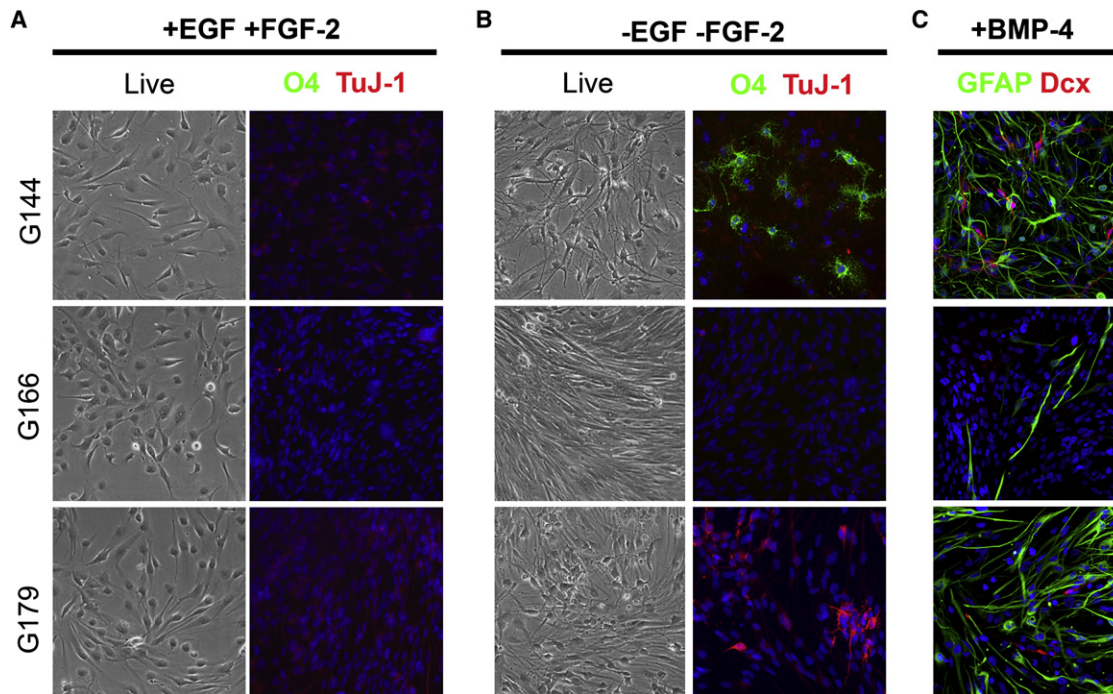
Figure 5. GNS Cell Lines Exhibit Distinct Differentiation Behavior

(A) In proliferating conditions (EGF and FGF-2), there is no detectable differentiation of G144, G166, or G179 cells into oligodendrocytes (green, O4^{+}) or neurons (red, TuJ-1^{+}).

(B) Seven days of growth factor withdrawal resulted in oligodendrocyte differentiation for G144 cultures, and G179 produced TuJ-1^{+} neurons.

(C) Following exposure to BMP-4 for 1 week, both G144 and G179 efficiently differentiate into GFAP^{+} cells, together with a minor population of Dcx[+] neuronal precursors. ("Live," phase-contrast image of live cultures).

Olig2, PDGFRα, and PDGFA than do other GNS cell lines and fetal NS cells. To verify that the observed marker heterogeneity was intrinsic to the GNS cells and not due to mixed populations, we generated clonal cell lines by single-cell deposition and assessed marker expression. For each line (n = 3), we saw heterogeneous expression of Olig2, Sox10, and NG2, similar to the parental line, and a capacity to generate oligodendrocytes upon growth factor withdrawal (Figure S6). G144 cells, therefore, stably exhibit an oligodendrocyte precursor-like phenotype prior to initiation of differentiation by growth factor withdrawal. Consistent with the oligodendrocyte differentiation in vitro, histopathological examination of sections from G144 xenograft tumors, including those generated from G144 clonal lines, identified cells with the typical "fried-egg" appearance indicative of an oligodendrocyte component (Figure S5). Furthermore, although diagnosed as a malignant astrocytoma (GBM), reexamination of the original patient tumor for G144 revealed a significant oligodendrocyte component based on histopathology and CNPase staining (Figures 3E and 3F).

GFAP is expressed in radial progenitors/radial glia in the developing primate nervous system, as well as in putative neural stem cells within the adult subventricular/subependymal zone (SVZ) (Levitt and Rakic, 1980; Doetsch et al., 1999). Human fetal NS cell lines express low levels of GFAP (Conti et al., 2005; Sun et al., 2008). Following BMP treatment, G179 cells upregulated GFAP (Figure 5C). However, prior to treatment, G179 cells express detectable levels of GFAP, in contrast to G144 cells,

which are predominantly negative. We assessed levels of an alternative splice form of GFAP, termed GFAPδ, which has been shown to mark human SVZ astrocytes (Roelofs et al., 2005). Expression of GFAPδ mRNA was greater than five times higher in G179 than in G144 and G166 (Figure 6B). Immunoblotting confirmed increased levels of protein (Figure 6C), and immunocytochemistry showed polymerized filaments of GFAPδ (Figure 6A). We find perinuclear enrichment of GFAPδ filaments similar to the staining reported for SVZ astrocytes in vivo (Roelofs et al., 2005). Levels of GFAPδ decrease following in vitro differentiation (Figure S7). We also identified GFAPδ-expressing cells within the original G179 patient tumor. These did not colocalize with CNPase-positive cells (Figure 6D). The coexpression of GFAPδ, Sox2, and Nestin and the ability to generate neuronal-like cells in vitro are features conserved with adult SVZ astrocytes (Sanai et al., 2004).

G166 cells lack expression of GFAPδ and OLP markers but do express CD44 and differentiate toward GFAP[+] astrocytes in vitro, suggesting a similarity to a more restricted astrocyte precursor. Together, these findings suggest that, despite their shared capacity to proliferate in response to EGF and FGF-2 and the widespread expression of neural progenitor markers, there are underlying differences between GNS cell lines. This may reflect relatedness to distinct subtypes of "normal" neural progenitor. These data further suggest that GFAPδ may be of use in discriminating astrocyte-like cells that have stem cell properties.
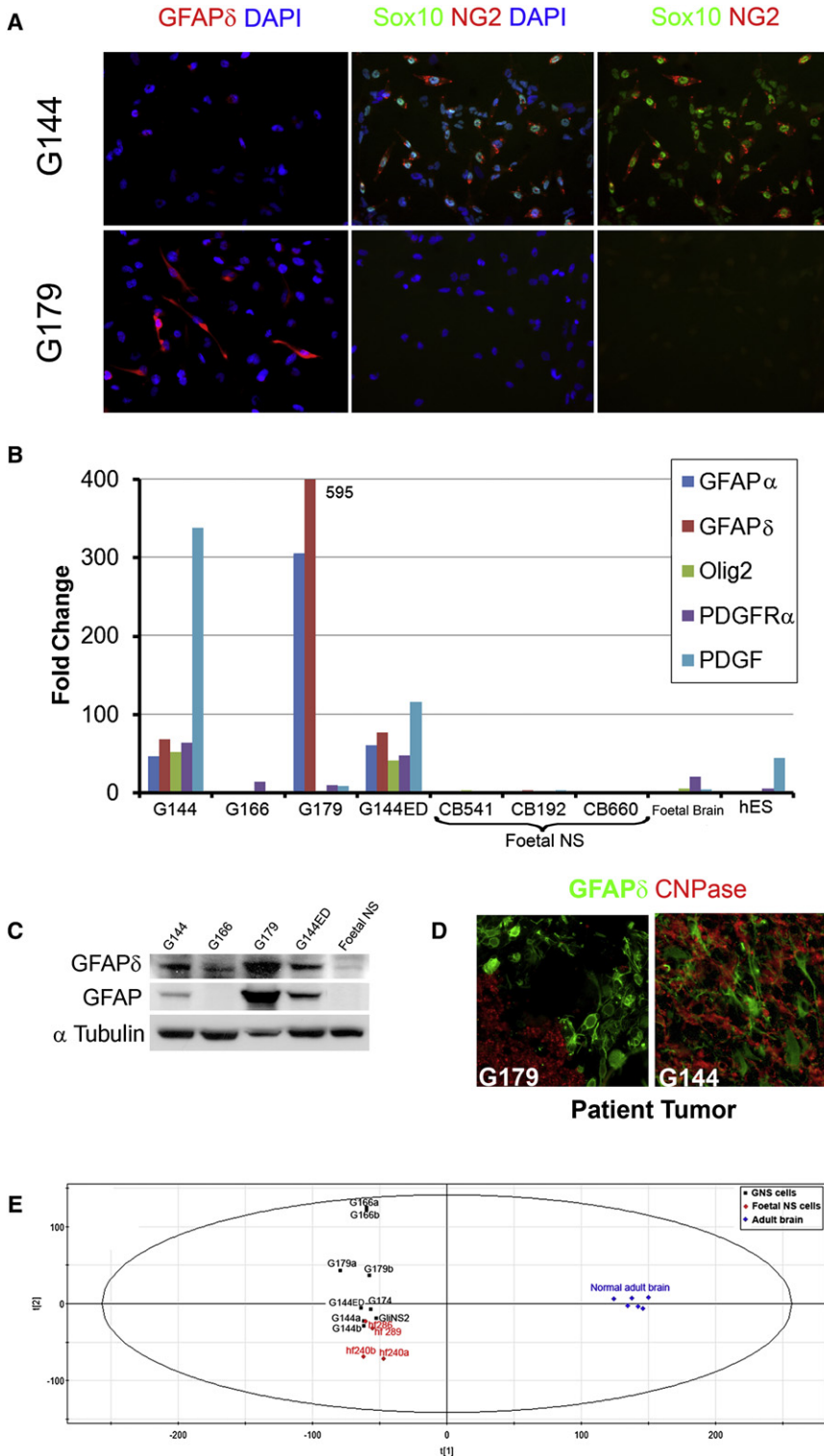
Figure 6. GNS Cells Express Lineage-Specific Characteristics

(A) Immunostaining in proliferating conditions identifies differential expression of lineage markers.

(B) Quantitative RT-PCR analysis. Control (hES) is a human embryonic stem cell line (hED1).

(C) Immunoblot for the adult SVZ astrocyte marker GFAPδ.

(D) GFAPδ-expressing cells in the original G179 patient tumor. The original G144 patient tumor contains large numbers of CNPase cells and cells with lower levels of GFAPδ.

(E) Principal component analysis (PCA) of global mRNA expression in each GNS cell line (black, G144, G144ED, G166, G179, G174, and GliNS2), fetal NS cells (red, hf240, hf286, and hf289), and normal adult brain tissue (blue). The "a" and "b" signify biological replicates.

state more closely related to fetal NS cells than to adult brain tissue (Figure 6E). Consistent with the previous analysis, we find that G179 and G166 have a distinct expression profile, both from one another and to G174, G144, and GliNS2.

We performed a cluster analysis using known NS cell and lineage-specific markers, as well as pathways known to be disrupted in gliomas (Figure S8). The dendrogram generated is similar to that for the global PCA analysis, indicating that this set of markers is sufficient to distinguish between lines. These data also confirmed that G144 expresses the OLP cell markers Sox8, Sox10, Olig1, Olig2, and Nkx2.2, whereas these are expressed at lower levels in G179, which has higher levels of GFAPδ. GliNS2 clusters closely with G144 and also expresses the OLP cell markers, suggesting that the phenotype of G144 may not be unique (Figure S8). Indeed, using immunostaining, we confirmed that GliNS2 expresses NG2, Olig2, and Sox10 and can generate oligodendrocytes readily upon growth factor withdrawal (Figure S9). G174 (derived from an oligoastrocytoma) did cluster closely to GliNS2 and G144, expressing higher levels of Olig2 and NG2. However, we failed to detect Sox10 protein by immunocytochemistry or oligodendrocyte differentiation (Figure S9). We found no evidence for expression of the pluripotency markers Oct4 or Nanog in any of the samples.

G166 shows higher levels of EGFR than any other line, perhaps explaining its resistance to differentiation upon EGF withdrawal

Comparison of mRNA Expression Profiles in GNS Cells

To evaluate the relationship between each GNS cell line and their correspondence to fetal NS cells, we carried out global mRNA expression profiling using microarrays. Principal component analysis reveals that each GNS cell line has a transcriptional

or BMP treatment. We also noted an apparent lack of mRNA for prominin-1 (CD133). Using flow cytometry, we examined the status of the cell surface markers CD133 and CD15/SSEA-1, which mark fetal and adult neural progenitors (Uchida et al., 2000; Capela and Temple, 2002) and also brain tumor-initiating cells (Singh et al., 2004). For G144 and G179, we observe heterogeneity for both markers within GNS cell cultures, similar to fetal NS cells (Sun et al., 2009), whereas G166 is negative, consistent with microarray expression data (Figure S10). We also found no evidence for CD133 expression within the original G166 tumor sample (data not shown). Lack of CD133 expression in certain glioma cell lines has also recently been described by Beier et al. (2007). By contrast, we find that, for each GNS cell line, including G166, the hyaluronic acid-binding protein CD44 is uniformly expressed. CD44 has previously been characterized as an astrocyte precursor marker, but we recently demonstrated that it also marks NS cells in vitro (Pollard et al., 2008). CD44 has been used to enrich for putative cancer stem cells in other types of solid cancer, such as breast, head and neck, and pancreas and prostate (Al-Hajj et al., 2003; Patrawala et al., 2006; Li et al., 2007; Prince et al., 2007).

To identify new candidate markers that distinguish fetal NS cells from GNS cells, we identified the most significantly differentially expressed transcripts across all six GNS cell lines versus three fetal NS cells. Genes located on chromosome 7 were significantly overrepresented within this set (Figure S11). This was not unexpected, given the variable copy number increases for this chromosome seen by SKY (Figure S2). The most significantly downregulated gene in GNS cells relative to fetal NS cells is the well-studied tumor suppressor PTEN, which is often lost or mutated in gliomas and other cancers (Louis, 2006). The top 100 differentially expressed genes (excluding those on chromosomes 7 or 19q) provide a set of candidate markers that distinguish GNS cells from nontumorigenic fetal NS cells (Figure S12).

Drug Screening Using Live Imaging of Adherent GNS Cells

The mouse neurosphere culture system has been used to screen compounds that affect neural stem cell expansion (Diamandis et al., 2007). However, there are several inherent limitations of this system. First, human neural stem cells expand more slowly in vitro than do their mouse counterparts. Quantification of cell proliferation is required for robust screening, which is difficult in suspension culture due to variable cell death. Second, neurospheres include restricted progenitors and differentiated cell types, and it is difficult to identify the precise cellular target. Third, real-time monitoring of cellular responses is not possible in aggregates. Finally, fusion of neurospheres is a common occurrence in suspension, which confounds analyses based solely on sphere numbers or size (Singec et al., 2006). Many of these hurdles are overcome using adherent monolayer GNS cells. Therefore, we undertook a proof-of-principle chemical screen using a live-cell imaging system (IncucyteHD) to monitor the effects of 450 compounds (NIH Clinical Collection). This collection comprises known drugs that have passed phase I–III trials and have been used in the clinic for various indications.

Following the addition of 10 μM of each drug, we captured live images of six parallel 96-well plates at 30 min intervals over a 2 day period. The relative change in confluence within each

individual well was measured at each time point. We carried out two independent screens using G144, G166, and G179, as well as a human fibroblast cell line (HS27). Thirty-eight drugs had significant cytotoxic or cytostatic effect on at least one line (Figures 7A–7C). Time-lapse movies of each well confirmed the effects of these compounds. Included within this set were drugs that disrupt core cell biological processes, including anthracycline chemotherapeutics (Doxorubicin and Idarubicin), the antimitotic Vindesine, and DNA topoisomerase inhibitors (Irinotecan and Etoposide) (Figure 7C). We also found line-specific effects for 15 compounds, consistent with the individualized phenotypes of GNS cells (Figure 7C).

We previously reported sensitivity of mouse neurospheres to perturbation of neurotransmitter pathways (Diamandis et al., 2007). Intriguingly, of the 23 drugs that killed all GNS cell lines, 7 are known to modulate the monoamine-signaling pathways. These are: two monoamine reuptake inhibitors (Indatraline and Paroxetine), a serotonin-specific reuptake inhibitor (Sertraline), two serotonin receptor agonists (CGS 12066B and Tegaserod), two dopamine receptor antagonists (10H-Phenothiazine and Trifluoperazine), and a dopamine transporter/sigma receptor modulator (Rimcazole). A monoamine oxidase inhibitor (Tryptoline) had a lesser but still detectable effect. Indatraline and Paroxetine had no effect on fibroblasts. Several of the drugs were validated using compounds obtained from an independent supplier (Figure 7D and Movies S13–S22). Interestingly, the addition of Indatraline, Rimcazole, or Sertraline resulted in cell death for all tumor lines and fetal NS cells but had less or no effect on the fibroblast cells. Following 1 hr exposure of GNS cells to Indatraline or Sertraline, active Caspase-3 and positive signal using the TUNEL assay were detected, confirming that cells undergo apoptosis (Figure 7E). Taken together, these results highlight the utility and scalability of adherent GNS cell lines for screening purposes and extend our previous findings, suggesting that brain cancer stem cells may be acutely sensitive to modulation of monoamine signaling and, particularly, the serotonin-signaling pathway.

DISCUSSION

Two critical unresolved issues relevant to the brain cancer stem cell hypothesis are: (1) how to maintain and expand pure populations of cancer stem cells and (2) elucidation of the phenotypic similarities between these cells and endogenous progenitors (Stiles and Rowitch, 2008). Here, we have demonstrated that pure populations of cancer stem cells can be expanded in vitro as cell lines using adherent culture methods previously established for fetal and human NS cells (Conti et al., 2005; Sun et al., 2008). Thus, suspension culture is not a requirement for successful long-term propagation of tumor-derived stem cells. In fact, by expanding glioma tumor-initiating cells as adherent cell lines, limitations of the neurosphere culture paradigm are overcome. Furthermore, whereas neurosphere culture yields expandable cultures from only a fraction of GBMs, our experience with adherent culture is that continuous stem cell lines have been obtained from all specimens that start with a reasonable cell viability. Increased levels of differentiation and apoptosis occur when GNS cells are cultured in suspension. It can be anticipated that sphere cultures will display a reduced
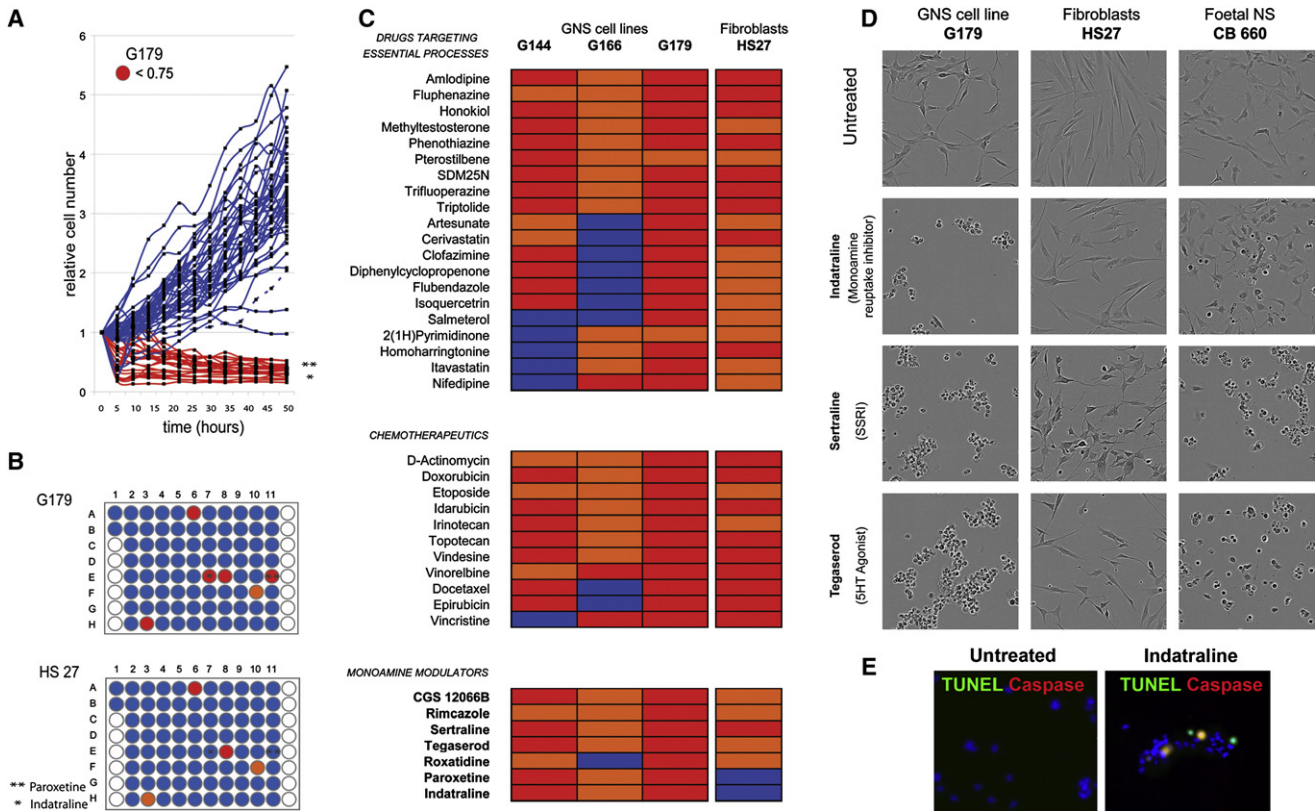
Figure 7. GNS Cells Are Suitable for Live Cell Imaging-Based Screens

(A) Relative cell number, derived from quantitative analyses of photomicrographs, is plotted against time for an example plate. In red are all of the "hits," compounds acting within the lowest 5th percentile, reducing cell number to < 0.75. Every tenth well for all other compounds is plotted in blue to illustrate the distribution range. Confluence readings after 2 days identify cytotoxic drugs. The Z factor for this screen was 0.76 (see Supplemental Experimental Procedures). The dotted blue line refers to Tryptoline.

(B) Cartoon of an example 96-well plate for GNS cell line G179 and HS27 (fibroblasts). Indatraline (*) and Paroxetine (**) show differential effects that affected all GNS cells, but not fibroblasts (HS27).

(C) Summary of active compounds. Red indicates compounds within the 5th percentile of cell confluence in two out of two screens; orange, in one of two screens; and blue, in neither of the two.

(D) To validate the results of the screen, we applied selected compounds from an independent source (2 μM for Tegaserod, 10 μM for all others) to G179 (left), HS 27 (middle), or fetal NS (right). Live images are shown after 2 days of treatment with each compound.

(E) Exposure of G179 cells to Indatraline induces apoptosis within 1 hr, as assessed by the TUNEL assay (green) and active caspase-3 (red).

tumorigenicity on a per cell basis compared to adherent GNS cultures, although side-by-side limiting dilution transplantation assays would be required to demonstrate this. Recently, Fael Al-Mayhani et al. (2009) reported high efficiency of deriving expandable glioma cultures using our adherent NS cell protocols, although they provide only preliminary molecular and phenotypic characterization.

Our findings indicate that gliomas are not driven by a single phenotype of tumor stem cell. In adherent GNS cell culture, tumor-specific stem cells can be distinguished based on lineage-specific markers. Within the developing and adult nervous system, there are several distinct classes of proliferative progenitors (e.g., neuroepithelial cells, radial glia, glial progenitors, oligodendrocyte progenitor cells, and SVZ astrocytes). G144 cells strongly express markers of the oligodendrocyte precursor cell/type C cell lineage and are biased toward oligodendrocyte differentiation. This phenotype is stable through passaging and is also observed in clonal cell lines. By contrast,

G179 appears more similar to adult SVZ astrocytes, including expression of GFAPδ, although more specific markers will be needed to confirm this. G166 cells are different again. Thus, the wide and continuous histological spectrum of gliomas with regard to proportions of the various differentiated and anaplastic cells may be dictated by the phenotype of the underlying tumor-initiating cells. As a larger set of GNS cell lines becomes available, we will be able to determine the frequency with which these distinct phenotypes occur and correlate precisely with primary tumor histopathology.

CD133 was not present on all GNS cell lines, confirming that this marker does not universally identify tumorigenic cells in malignant glioma (Beier et al., 2007). Glioblastoma-derived neurospheres are reported to fall into two distinct groups based on their adhesion properties (Gunther et al., 2007). However, markers that specifically distinguish these two categories of culture have not been described. Therefore, their correspondence to the GNS cell lines cannot readily be ascertained (Figure S13).

Our data would be consistent with tumor stem cells arising following transformation of OLPs or adult SVZ astrocytes. However, it is equally plausible that short-lived progenitors or differentiated cells can be converted to a stem cell state through genetic/epigenetic disruptions. Indeed, OLPs in vitro can acquire stem cell properties through sequential exposure to BMP, PDGF, and EGF/FGF (Kondo and Raff, 2000).

GNS cells can be genetically modified, enabling sophisticated chemical or genetic screens—for example, incorporating fluorescent reporters. We have also demonstrated their utility for morphometric analysis of cell behavior and tracking of cell motility, an important feature of malignant gliomas (Dirks, 2001). They should also be amenable to lineage-tracing experiments, as recently reported for fetal CNS progenitor cultures (Ravin et al., 2008). Suspension culture methodology is currently favored for propagation of cells from a range of solid tumors, such as breast (Liao et al., 2007) and colon cancer (Ricci-Vitiani et al., 2007). We suggest that, where possible, derivation of adherent stem cell lines could offer significant advantages.

We demonstrated proof of principle of the utility of GNS cells by carrying out a small-scale chemical screen of known pharmaceutical drugs. The findings extend to human brain cancer stem cells our observation that mouse neurospheres are sensitive to modulation of neurotransmitter pathways (Diamandis et al., 2007). Future studies will determine whether those drugs that modulate the serotonin pathway can limit growth of xenograft tumors in vivo.

In conclusion, GNS cells provide a versatile and renewable resource to probe the biology of tumor-initiating cells and screen for agents that selectively and directly target them. Tumor stem cell self-renewal, migration, apoptosis, and differentiation all represent potential therapeutic opportunities that are accessible in GNS cell cultures.

EXPERIMENTAL PROCEDURES

Tumor Samples and Cell Culture

Brain tumor samples were obtained following local ethical board approval. G144 and G144ED (51-year-old male), G166 (74-year-old female), and GliNS2 (54-year-old male) were diagnosed as classic glioblastoma multiform (GBM). G179 (56-year-old male) was a GBM (giant cell variant). G174 (60-year-old male) was an anaplastic oligodendroglioma. Tumors were dissociated into single cells by placing in Accutase (Sigma) or an enzyme cocktail for 15–20 min at 37°C (Singh et al., 2003). For those tumors with excess debris, cells were initially allowed to form spheres/aggregates in suspension culture, and these were then transferred to a fresh laminin-coated flask. They subsequently attached and began to outgrow over the course of a week.

Culture of GNS Cells

GNS cell expansion was carried out using serum-free media supplemented with N2, B27, EGF, and FGF-2 (20 ng/ml), as described previously for human fetal NS cells (Sun et al., 2008). Culture vessels were coated with Laminin (Sigma) for 3 hr at 10 ug/ml prior to use. GNS cells were routinely grown to confluence, dissociated using Accutase (Sigma), and then split 1:3 to 1:5. Medium was replaced every 3–5 days. Foetal NS cells CB541 and CB660 have been described previously (Sun et al., 2008), and hf240, hf286, and hf289 were isolated using similar techniques (I.C., unpublished data). GNS cell lines have been deposited in the ATTC and can be requested from the cell repository at Biorep (Milan, Italy). For differentiations, we used laminin-coated 4-well plates (∼0.5 −1 × 10^5 cells/well) (Nunc) or 24-well Imagelock microplates (Essen Instruments). For oligodendrocytes and neuronal differentiation, we used the same basal media but lacking EGF or FGF-2 (i.e., growth

factor withdrawal). For astrocyte differentiation, we added BMP at 10 ng/ml (R and D Systems). A detailed protocol is available in the Supplemental Experimental Procedures.

Genomic Analysis

Cultures were colcemid treated for cytogenetic harvest. Spectral Karyotyping (SKY) was performed using the commercially available kit provided by Applied Spectral Imaging (Vista, CA). Slides were imaged and analyzed by fluorescent microscope. For CGH analysis, 1.5 ug genomic DNA was prepared using Wizard genomic DNA extraction kit (Promega). Sample preparation, CGH hybridization, and analysis were performed using human 4 × 44 k CGH microarrays, feature extraction, and CGH analytics software (Agilent). Significant chromosomal aberrations have been determined using algorithm ADM-2 (window = 5 kb; threshold = 15.5).

Fluorescence In Situ Hybridization

Fluorescence in situ hybridization (FISH) was performed on cytogenetic preparations or formalin-fixed paraffin-embedded (FFPE) sections using the Centromere 7-specific and EGFR-locus-specific FISH probes provided by Vysis (Abbott Technologies).

Immunocytochemistry

Immunocytochemistry was performed as described previously (Conti et al., 2005). Primary antibodies: human Nestin (1:500), O4 (1:100, live stain), and Sox2 (1:50) (R and D Systems); Vimentin (1:50), 3CB2 (1:20) (DSHB, University of Iowa), and TuJ-1 (1:500) (Covance); CD44 (1:100, live stain) (E-bioscience); GFAP (1:300) (Sigma, monoclonal GA-5); and NG2 (1:100), Olig2 (1:200), and GFAPδ (1:200) (Chemicon). We used goat secondary antibodies conjugated to Alexa dyes, 1:1000 (Molecular Probes). For analysis of apoptosis, we treated cells with either DMSO (0.1%) or Indatraline 10 uM or Sertraline 10 uM. After 1 hr treatment, cells were fixed for 30 min with 4% PFA and were permeabilized with Triton X-100 and sodium citrate 0.1%. Cells were then assessed using the TUNEL assay (In Situ Cell Death Detection kit, Roche) and subsequently processed for immunocytochemistry using an anti active Caspase-3 antibody (BD PharMingen). DAPI was used as nuclear counterstain (Sigma). Images were acquired using a Leica DMI400B inverted fluorescence microscope linked to a DFC340FX camera.

Flow Cytometry

We used the following antibodies: CD133 (1:5) (Miltenyi), CD15 (1:100) (BD), and CD44-PE/Cy5 (1:1000) (eBioscience). Clonal cell lines were established using a flow sorter (MoFlo, Dako) to deposit single cells into each well of a 96-well plate.

Mouse Brain Fixation, Histopathology, and Immunohistochemistry

These procedures were carried out as described (Singh et al., 2004). Antibody staining was carried out following deparaffinisation and heat-induced antigen retrieval using citrate buffer (pH 6.0). The antibodies used were CNPase 1:200 (Sigma), hNestin 1:200 (Millipore), hGFAP 1:200 (Sternberger monoclonals), and GFAP-δ, 1:500 (Millipore).

Xenotransplantation

GNS cells were injected stereotactically into 6- to 8-week-old NOD-SCID mouse frontal cortex, following administration of general anesthesia. Details are available in the Supplemental Experimental Procedures.

Microarrays and Bioinformatics

Expression profiling was carried out using the GeneChip Human Genome U133 Plus 2.0 Array (Affymetrix). Data were preprocessed using Bioconductor packages: affyQCReport for quality control checks and the vsnrma function of the Bioconductor package vsn for data normalization. The limma package in Bioconductor was used for statistically analyzing the data using both the modified t test and f test and the false discovery rate (FDR) method for multiple hypothesis correction. Dendograms and heatmap plots were created using the hclust package in Bioconductor. Hierarchical clustering (using the Euclidean distance and the average linkage method) was performed on the normalized data set and then on various lists of statistically significant differentially expressed genes. Umetrics software was used to perform a principal

components analysis (PCA) on the normalized data set, and partial least square discriminant analysis (PLS-DA) was used to determine group classifiers. The Web-based tool GeneTrail (http://genetrail.bioinf.uni-sb.de/) was used to perform both overrepresentation analysis and gene set enrichment analysis. Array data are available from the NIH Gene Expression Omnibus (accession number GSE15209).

Quantitative RT-PCR
Total mRNA was harvested using the QIAGEN RNeasy kit (QIAGEN). cDNA was generated using Superscript III (Invitrogen), and quantitative PCR was carried out using the LightCycler system (Roche). Data presented here are means of biological and technical duplicates. Samples were normalized using β-actin primers, and the data are expressed relative to fetal NS cell (CB660) expression. Primers were designed using Primer 3 software (MIT): GFAPδF ACATCGAGATCGCCACCTAC; GFAPδR, CGGCGTTCCATTTACAATCT; GFAPαF, ACATCGAGATCGCCACCTAC; GFAPαR, ATCTCCACGGTCTTCAC CAC; PDGFRαF, CCACCGTCAAAGGAAAGAAG; PDGFRαR, CCAATTTGAT GGATGGGACT; PDGFAF, GATACCTCGCCCATGTTCTG; PDGFAR, CAGG CTGGTGTCCAAAGAAT; Olig2F, CAGAAGCGCTGATGG; and Olig2R, TCG GCAGTTTTGGGT.

Immunoblotting
A 10% protein gel (Invitrogen) was used, and blotting was performed using the iBlot Dry Blotting system (Invitrogen). Antibodies were anti-α-tubulin antibody at 1:5000 (Abcam), anti-GFAPδ 1:500 (Chemicon), and GFAP 1:500 (Sigma). Secondary antibody conjugated to HRP was used with the ECL system to detect protein (Amersham).

Time-Lapse Movies and Drug Screening
For routine time-lapse imaging and generation of growth curves, we used the Incucyte system (Essen Instruments, USA). For cell tracking analysis, we processed image stacks using ImageJ and analyzed cell tracks using the MTrackJ Plugin (http://rsb.info.nih.gov/ij/).

We used the NIH clinical collection of 480 compounds (www.nihclinicalcollection.com). The IncucyteHD system (Essen Instruments, USA) enables simultaneous monitoring of six 96-well microplates. GNS cell lines were plated at 10%–20% confluence on 96-well plates (Iwaki). Compounds were added to the plates at a final concentration of 10 μM per compound per well (DMSO 0.1%). Relative increase in cell number values was generated for every well using confluence readings obtained at each time point relative to the starting confluence. For every cell line (G144, G166, G179, and HS27), two independent screens were run. HS27 is a human foreskin fibroblast line (American Type Culture Collection). Every well associated with a reduction in cell number within the 5th percentile in at least two independent screens was visually inspected. For validation, a few chosen compounds were received from an independent supplier—Indatraline, Rimcazole, and Sertraline (Sigma) and Tegaserod (Sequoia Research Products)—and a similar set of experiments was conducted in 24 wells with 2 μM or 10 μM of compound.

ACCESSION NUMBERS
The Affymetrix microarray data have been deposited in the NIH Gene Expression Omnibus with accession number GSE15209.

SUPPLEMENTAL DATA
Supplemental Data include Supplemental Experimental Procedures, 13 figures, 1 table, and 22 movies and can be found with this article online at http://www.cell.com/cell-stem-cell/supplemental/S1934-5909(09)00149-0.

REFERENCES

Al-Hajj, M., Wicha, M.S., Benito-Hernandez, A., Morrison, S.J., and Clarke, M.F. (2003). Prospective identification of tumorigenic breast cancer cells. Proc. Natl. Acad. Sci. USA 100, 3983–3988.

Beier, D., Hau, P., Proescholdt, M., Lohmeier, A., Wischhusen, J., Oefner, P.J., Aigner, L., Brawanski, A., Bogdahn, U., and Beier, C.P. (2007). CD133(+) and CD133(−) glioblastoma-derived cancer stem cells show differential growth characteristics and molecular profiles. Cancer Res. 67, 4010–4015.

Cancer Genome Atlas Research Network. (2008). Comprehensive genomic characterization defines human glioblastoma genes and core pathways. Nature 455, 1061–1068.

Capela, A., and Temple, S. (2002). LeX/ssea-1 is expressed by adult mouse CNS stem cells, identifying them as nonependymal. Neuron 35, 865–875.

Conti, L., Pollard, S.M., Gorba, T., Reitano, E., Toselli, M., Biella, G., Sun, Y., Sanzone, S., Ying, Q.L., Cattaneo, E., et al. (2005). Niche-independent symmetrical self-renewal of a mammalian tissue stem cell. PLoS Biol. 3, e283.

Diamandis, P., Wildenhain, J., Clarke, I.D., Sacher, A.G., Graham, J., Bellows, D.S., Ling, E.K., Ward, R.J., Jamieson, L.G., Tyers, M., et al. (2007). Chemical genetics reveals a complex functional ground state of neural stem cells. Nat. Chem. Biol. 3, 268–273.

Dirks, P.B. (2001). Glioma migration: Clues from the biology of neural progenitor cells and embryonic CNS cell migration. J. Neurooncol. 53, 203–212.

Doetsch, F., Caille, I., Lim, D.A., Garcia-Verdugo, J.M., and Alvarez-Buylla, A. (1999). Subventricular zone astrocytes are neural stem cells in the adult mammalian brain. Cell 97, 703–716.

Doetschman, T.C., Eistetter, H., Katz, M., Schmidt, W., and Kemler, R. (1985). The in vitro development of blastocyst-derived embryonic stem cell lines: Formation of visceral yolk sac, blood islands and myocardium. J. Embryol. Exp. Morphol. 87, 24–45.

Fael Al-Mayhani, T.M., Ball, S.L., Zhao, J.W., Fawcett, J., Ichimura, K., Collins, P.V., and Watts, C. (2009). An efficient method for derivation and propagation of glioblastoma cell lines that conserves the molecular profile of their original tumours. J. Neurosci. Methods 176, 192–199.

Furnari, F.B., Fenton, T., Bachoo, R.M., Mukasa, A., Stommel, J.M., Stegh, A., Hahn, W.C., Ligon, K.L., Louis, D.N., Brennan, C., et al. (2007). Malignant astrocytic glioma: Genetics, biology, and paths to treatment. Genes Dev. 21, 2683–2710.

Galli, R., Binda, E., Orfanelli, U., Cipelletti, B., Gritti, A., De Vitis, S., Fiocco, R., Foroni, C., Dimeco, F., and Vescovi, A. (2004). Isolation and characterization of tumorigenic, stem-like neural precursors from human glioblastoma. Cancer Res. 64, 7011–7021.

Glaser, T., Pollard, S.M., Smith, A., and Brustle, O. (2007). Tripotential differentiation of adherently expandable neural stem (NS) cells. PLoS ONE 2, e298.

Gunther, H.S., Schmidt, N.O., Phillips, H.S., Kemming, D., Kharbanda, S., Soriano, R., Modrusan, Z., Meissner, H., Westphal, M., and Lamszus, K. (2007). Glioblastoma-derived stem cell-enriched cultures form distinct subgroups according to molecular and phenotypic criteria. Oncogene 27, 2897–2909.

Hemmati, H.D., Nakano, I., Lazareff, J.A., Masterman-Smith, M., Geschwind, D.H., Bronner-Fraser, M., and Kornblum, H.I. (2003). Cancerous stem cells can arise from pediatric brain tumors. Proc. Natl. Acad. Sci. USA 100, 15178–15183.

Ignatova, T.N., Kukekov, V.G., Laywell, E.D., Suslov, O.N., Vrionis, F.D., and Steindler, D.A. (2002). Human cortical glial tumors contain neural stem-like cells expressing astroglial and neuronal markers in vitro. Glia 39, 193–206.

Kleihues, P., and Cavenee, W.K. (2000). Pathology and Genetics: Tumours of the Nervous System (Lyon: IARC Press).

Kondo, T., and Raff, M. (2000). Oligodendrocyte precursor cells reprogrammed to become multipotential CNS stem cells. Science 289, 1754–1757.

Lapidot, T., Sirard, C., Vormoor, J., Murdoch, B., Hoang, T., Caceres-Cortes, J., Minden, M., Paterson, B., Caligiuri, M.A., and Dick, J.E. (1994). A cell initiating human acute myeloid leukaemia after transplantation into SCID mice. Nature 367, 645–648.

Lee, J., Kotliarova, S., Kotliarov, Y., Li, A., Su, Q., Donin, N.M., Pastorino, S., Purow, B.W., Christopher, N., Zhang, W., et al. (2006). Tumor stem cells derived from glioblastomas cultured in bFGF and EGF more closely mirror the phenotype and genotype of primary tumors than do serum-cultured cell lines. Cancer Cell 9, 391–403.

Levitt, P., and Rakic, P. (1980). Immunoperoxidase localization of glial fibrillary acidic protein in radial glial cells and astrocytes of the developing rhesus monkey brain. J. Comp. Neurol. 193, 815–840.

Li, C., Heidt, D.G., Dalerba, P., Burant, C.F., Zhang, L., Adsay, V., Wicha, M., Clarke, M.F., and Simeone, D.M. (2007). Identification of pancreatic cancer stem cells. Cancer Res. 67, 1030–1037.

Liao, M.J., Zhang, C.C., Zhou, B., Zimonjic, D.B., Mansi, S.A., Kaba, M., Gifford, A., Reinhardt, F., Popescu, N.C., Guo, W., et al. (2007). Enrichment of a population of mammary gland cells that form mammospheres and have in vivo repopulating activity. Cancer Res. 67, 8131–8138.

Louis, D.N. (2006). Molecular pathology of malignant gliomas. Annu. Rev. Pathol. 1, 97–117.

Mischel, P.S., Shai, R., Shi, T., Horvath, S., Lu, K.V., Choe, G., Seligson, D., Kremen, T.J., Palotie, A., Liau, L.M., et al. (2003). Identification of molecular subtypes of glioblastoma by gene expression profiling. Oncogene 22, 2361–2373.

Parsons, D.W., Jones, S., Zhang, X., Lin, J.C., Leary, R.J., Angenendt, P., Mankoo, P., Carter, H., Siu, I.M., Gallia, G.L., et al. (2008). An integrated genomic analysis of human glioblastoma multiforme. Science 321, 1807–1812.

Patrawala, L., Calhoun, T., Schneider-Broussard, R., Li, H., Bhatia, B., Tang, S., Reilly, J.G., Chandra, D., Zhou, J., Claypool, K., et al. (2006). Highly purified CD44(+) prostate cancer cells from xenograft human tumors are enriched in tumorigenic and metastatic progenitor cells. Oncogene 25, 1696–1708.

Phillips, H.S., Kharbanda, S., Chen, R., Forrest, W.F., Soriano, R.H., Wu, T.D., Misra, A., Nigro, J.M., Colman, H., Soroceanu, L., et al. (2006). Molecular subclasses of high-grade glioma predict prognosis, delineate a pattern of disease progression, and resemble stages in neurogenesis. Cancer Cell 9, 157–173.

Pollard, S.M., Conti, L., Sun, Y., Goffredo, D., and Smith, A. (2006). Adherent neural stem (NS) cells from fetal and adult forebrain. Cereb. Cortex 16 (Suppl 1), i112–i120.

Pollard, S.M., Wallbank, R., Tomlinson, S., Grotewold, L., and Smith, A. (2008). Fibroblast growth factor induces a neural stem cell phenotype in foetal forebrain progenitors and during embryonic stem cell differentiation. Mol. Cell. Neurosci. 38, 393–403.

Prince, M.E., Sivanandan, R., Kaczorowski, A., Wolf, G.T., Kaplan, M.J., Dalerba, P., Weissman, I.L., Clarke, M.F., and Ailles, L.E. (2007). Identification of a subpopulation of cells with cancer stem cell properties in head and neck squamous cell carcinoma. Proc. Natl. Acad. Sci. USA 104, 973–978.

Ravin, R., Hoeppner, D.J., Munno, D.M., Carmel, L., Sullivan, J., Levitt, D.L., Miller, J.L., Athaide, C., Panchision, D.M., and McKay, R.D. (2008). Potency and fate specification in CNS stem cell populations in vitro. Cell Stem Cell 3, 670–680.

Reya, T., Morrison, S.J., Clarke, M.F., and Weissman, I.L. (2001). Stem cells, cancer, and cancer stem cells. Nature 414, 105–111.

Reynolds, B.A., and Rietze, R.L. (2005). Neural stem cells and neurospheres—re-evaluating the relationship. Nat. Methods 2, 333–336.

Ricci-Vitiani, L., Lombardi, D.G., Pilozzi, E., Biffoni, M., Todaro, M., Peschle, C., and De Maria, R. (2007). Identification and expansion of human colon-cancer-initiating cells. Nature 445, 111–115.

Roelofs, R.F., Fischer, D.F., Houtman, S.H., Sluijs, J.A., Van Haren, W., Van Leeuwen, F.W., and Hol, E.M. (2005). Adult human subventricular, subgranular, and subpial zones contain astrocytes with a specialized intermediate filament cytoskeleton. Glia 52, 289–300.

Sanai, N., Tramontin, A.D., Quinones-Hinojosa, A., Barbaro, N.M., Gupta, N., Kunwar, S., Lawton, M.T., McDermott, M.W., Parsa, A.T., Manuel-Garcia Verdugo, J., et al. (2004). Unique astrocyte ribbon in adult human brain contains neural stem cells but lacks chain migration. Nature 427, 740–744.

Singec, I., Knoth, R., Meyer, R.P., Maciaczyk, J., Volk, B., Nikkhah, G., Frotscher, M., and Snyder, E.Y. (2006). Defining the actual sensitivity and specificity of the neurosphere assay in stem cell biology. Nat. Methods 3, 801–806.

Singh, S.K., Clarke, I.D., Terasaki, M., Bonn, V.E., Hawkins, C., Squire, J., and Dirks, P.B. (2003). Identification of a cancer stem cell in human brain tumors. Cancer Res. 63, 5821–5828.

Singh, S.K., Hawkins, C., Clarke, I.D., Squire, J.A., Bayani, J., Hide, T., Henkelman, R.M., Cusimano, M.D., and Dirks, P.B. (2004). Identification of human brain tumour initiating cells. Nature 432, 396–401.

Stiles, C.D., and Rowitch, D.H. (2008). Glioma stem cells: A midterm exam. Neuron 58, 832–846.

Sun, Y., Pollard, S., Conti, L., Toselli, M., Biella, G., Parkin, G., Willatt, L., Falk, A., Cattaneo, E., and Smith, A. (2008). Long-term tripotent differentiation capacity of human neural stem (NS) cells in adherent culture. Mol. Cell. Neurosci. 38, 245–258.

Sun, Y., Kong, W., Falk, A., Hu, J., Zhou, L., Pollard, S., and Smith, A. (2009). CD133 (Prominin) negative human neural stem cells are clonogenic and tripotent. PLoS ONE 4, e5498.

Suslov, O.N., Kukekov, V.G., Ignatova, T.N., and Steindler, D.A. (2002). Neural stem cell heterogeneity demonstrated by molecular phenotyping of clonal neurospheres. Proc. Natl. Acad. Sci. USA 99, 14506–14511.

Uchida, N., Buck, D.W., He, D., Reitsma, M.J., Masek, M., Phan, T.V., Tsukamoto, A.S., Gage, F.H., and Weissman, I.L. (2000). Direct isolation of human central nervous system stem cells. Proc. Natl. Acad. Sci. USA 97, 14720–14725.

Ward, R.J., and Dirks, P.B. (2007). Cancer stem cells: At the headwaters of tumor development. Annu. Rev. Pathol. 2, 175–189.

Yuan, X., Curtin, J., Xiong, Y., Liu, G., Waschsmann-Hogiu, S., Farkas, D.L., Black, K.L., and Yu, J.S. (2004). Isolation of cancer stem cells from adult glioblastoma multiforme. Oncogene 23, 9392–9400.